RESEARCH ARTICLE

Special Section:
Global Land-Use Change and Carbon/Climate Dynamics

Key Points:
- The uncertainty in the net LULCC flux due to model parameterization is large
- Tree cover is a critical factor in the quantification of the LULCC flux
- The practice of calibrating the net land carbon balance limits the applicability of an ESM

Supporting Information:
- Supporting Information S1–S4
- Figure S1
- Figure S2a
- Figure S2b
- Figure S2c
- Figure S2d
- Figure S3a
- Figure S3b
- Figure S3c
- Figure S4

Correspondence to:
D. S. Goll,
daniel.goll@lsce.ipsl.fr

Strong dependence of CO$_2$ emissions from anthropogenic land cover change on initial land cover and soil carbon parametrization

Daniel S. Goll[1,2,3], Victor Brovkin[1], Jari Liski[4], Thomas Raddatz[1], Tea Thum[5], and Kathe E. O. Todd-Brown[6,7]

[1]Land in the Earth System, Max Planck Institute for Meteorology, Hamburg, Germany, [2]KlimaCampus, Hamburg, Germany, [3]Now at Laboratoire des Sciences du Climat et de l'Environnment, CEA, CNRS, UVSQ, Gif-sur-Yvette, France, [4]Finnish Environment Institute (SYKE), Helsinki, Finland, [5]Finnish Meteorological Institute, Helsinki, Finland, [6]Department of Microbiology and Plant Biology, University of Oklahoma, Norman, Oklahoma, USA, [7]Now at Biological Sciences Division, Pacific Northwest National Laboratory, Richland, Washington, USA

Abstract The quantification of sources and sinks of carbon from land use and land cover changes (LULCC) is uncertain. We investigated how the parametrization of LULCC and of organic matter decomposition, as well as initial land cover, affects the historical and future carbon fluxes in an Earth System Model (ESM). Using the land component of the Max Planck Institute ESM, we found that the historical (1750–2010) LULCC flux varied up to 25% depending on the fraction of biomass which enters the atmosphere directly due to burning or is used in short-lived products. The uncertainty in the decadal LULCC fluxes of the recent past due to the parametrization of decomposition and direct emissions was 0.6 Pg C yr^{-1}, which is 3 times larger than the uncertainty previously attributed to model and method in general. Preindustrial natural land cover had a larger effect on decadal LULCC fluxes than the aforementioned parameter sensitivity (1.0 Pg C yr^{-1}). Regional differences between reconstructed and dynamically computed land covers, in particular, at low latitudes, led to differences in historical LULCC emissions of 84–114 Pg C, globally. This effect is larger than the effects of forest regrowth, shifting cultivation, or climate feedbacks and comparable to the effect of differences among studies in the terminology of LULCC. In general, we find that the practice of calibrating the net land carbon balance to provide realistic boundary conditions for the climate component of an ESM hampers the applicability of the land component outside its primary field of application.

1. Introduction

Land use and land cover changes (LULCC) are significant drivers of atmospheric CO$_2$ concentration. The assessment of uncertainties in sources and sinks of carbon from LULCC is crucial for a better understanding of the terrestrial carbon balance. Previous studies have shown that the large uncertainty in carbon fluxes connected to LULCC are attributed to the available data on land cover change, the simplified and incomplete description of biological and LULCC processes in models, and the inconsistent use of definitions of LULCC [*Houghton et al.*, 2012; *Pongratz et al.*, 2014]. However, the relative contribution of each aspect remains elusive.

Earth system models (ESMs) and their precursors are a common tool to quantify LULCC emissions and feedbacks between LULCC and climate [*Strassmann et al.*, 2008; *Pitman et al.*, 2009; *Arora and Boer*, 2010; *de Noblet-Ducoudré et al.*, 2012; *Houghton et al.*, 2012; *Lawrence et al.*, 2012; *Pitman et al.*, 2012; *Brovkin et al.*, 2013a; *Shevliakova et al.*, 2013]. ESMs incorporate process-based land components, land surface models (LSMs), which integrate biological, hydrological, and physical processes within the soil-plant-atmosphere continuum [*Prentice et al.*, 2014]. A LSM often used in LULCC studies is Jena Scheme for Biosphere-Atmosphere Coupling in Hamburg (JSBACH), the land component of the Max Planck Institute Earth System Model (MPI-ESM) [*Giorgetta et al.*, 2013]. It was used to study the biogeochemical [*Pongratz et al.*, 2009a], the biogeophysical [*Pongratz et al.*, 2009b; *Pitman et al.*, 2009; *de Noblet-Ducoudré et al.*, 2012; *Brovkin et al.*, 2013a], or the combined [*Pongratz et al.*, 2010, 2011; *Pitman et al.*, 2012] climate responses, as well as to quantify changes in the terrestrial carbon balance [*Reick et al.*, 2010; *Houghton et al.*, 2012; *Reick et al.*, 2013; *Wilkenskjeld et al.*, 2014; *Schneck et al.*, 2015].

The version of MPI-ESM used in the Coupled Model Intercomparison Project Phase 5 (CMIP5) overestimates emissions due to LULCC compared to other ESMs [*Brovkin et al.*, 2013a], LSMs, and bookkeeping approaches [*Houghton et al.*, 2012], although lower emissions were simulated by its precursor European Center/Hamburg Model 5 (ECHAM5)/JSBACH [*Pongratz et al.*, 2009a; *Reick et al.*, 2010]: accumulated LULCC emissions between 1850 and 2005 differ by a factor of 2 between MPI-ESM and ECHAM5/JSBACH. Importantly, this difference could not be explained by two modifications of the representation of LULCC in MPI-ESM which are not present in its precursor. The first modification, the representation of annual gross land cover changes, resolving land use practices like shifting cultivation, lead to an increase in historical emission by less than 40% compared to treating LULCC as the net change in cover from one year to the next [*Wilkenskjeld et al.*, 2014]. The second modification, the inclusion of interactions between LULCC and changes in natural land cover, was shown to have a negligible effect on historical LULCC emissions [*Schneck et al.*, 2015].

To pin down the causes of the large difference in the net LULCC flux between model versions, we investigate the major constraints on the simulated net LULCC flux for a given LULCC scenario. Theoretically, the primary constraint on the emissions from LULCC on centennial timescale is the initial land cover, as the biomass density connected to the cover types determines the potential for emissions. On shorter timescale, the evolution of the emissions depends on the fraction of carbon released directly after LULCC to the atmosphere (direct emissions), for example, when a forest is cleared by fire, and on the turnover of decomposing biomass (legacy emissions). In the following we will discuss the rationale to select these processes as major constraints on the net LULCC flux in more detail.

Initial land cover is critical to LULCC emissions [*McGuire et al.*, 2001; *Houghton et al.*, 2012] but challenging to reconstruct [*Ramankutty et al.*, 2007]. Due to the higher carbon density, the conversion of a forest into agricultural land by deforestation leads to much higher emissions than the conversion of a natural grassland into agricultural land. The state-of-the-art data on land cover change by *Hurtt et al.* [2011] contain no information on the type of natural vegetation which is converted. Thus, the effect of land cover changes on the carbon balance depends on the assumed initial land cover.

There is a trend to compute natural land cover dynamically according to climate instead of treating it fixed [*Cox*, 2001; *Krinner et al.*, 2005; *Sato et al.*, 2007; *Watanabe et al.*, 2011; *Delworth et al.*, 2012; *Brovkin et al.*, 2013b; *Dunee et al.*, 2013; *Ji et al.*, 2014]. These models are shown to be able to reasonably well replicate present-day land cover [*Sitch et al.*, 2003; *Brovkin et al.*, 2013b]. However, they lack mechanistic representations of vegetation dynamics as, for example, establishment and mortality, resulting in the need of periodic recalibration to changes in the terrestrial and atmospheric components of the ESM. Furthermore, the model evaluation is severely hampered by lack of appropriate data [*Houghton et al.*, 2012; *Reick et al.*, 2013]. Even though biases in the land cover simulated by MPI-ESM are known [*Brovkin et al.*, 2013b], it has not been addressed how far they affect the net LULCC flux and other carbon fluxes [*Brovkin et al.*, 2013a; *Reick et al.*, 2013; *Schneck et al.*, 2015; *Wilkenskjeld et al.*, 2014].

Direct carbon emissions, due to burning or anthropocentric use in short-lived products, is a key short-term driver of LULCC emissions [*Ramankutty et al.*, 2007; *Houghton et al.*, 2012]. In global models, fixed fractions of direct emission are used [*McGuire et al.*, 2001; *Pongratz et al.*, 2009a; *Arora and Boer*, 2010; *Watanabe et al.*, 2011], which are usually derived from early work by *Houghton et al.* [1983]. However, these fractions are poorly constrained by observations [*Fearnside*, 2000; *Ramankutty et al.*, 2007; *van der Werf*, 2010]. In MPI-ESM the parameter controlling the fraction of direct emission was chosen arbitrarily as it was argued to be irrelevant for multicentennial emissions, for which the LULCC model was initially designed [*Pongratz et al.*, 2009b]. However, the model was subsequently applied to much shorter timescales [*Pitman et al.*, 2012; *Houghton et al.*, 2012; *Brovkin et al.*, 2013a; *Giorgetta et al.*, 2013; *Reick et al.*, 2013; *Wilkenskjeld et al.*, 2014], and this fraction was recalibrated to minimize biases in the historical land carbon balance [*Giorgetta et al.*, 2013]. Although the parametrization of direct emissions controls legacy emissions, a global quantification of this uncertainty is missing.

Long-term LULCC emissions are primarily controlled by decomposition and, to a lesser extent, by changes in plant productivity and biomass turnover due replacement of naturally occurring vegetation with crops. Up to 60% of current LULCC emissions are attributed to LULCC in the past, showing the large influence of legacy emissions on present fluxes from tropics [*Ramankutty et al.*, 2007]. Similarly, *Reick et al.* [2010] found that the same land cover change data resulted in 40% less emissions in the period 1850 to 1990 in a comprehensive model compared to a bookkeeping approach. The difference between model and bookkeeping approach

was almost entirely explained by different treatment of decomposition [*Reick et al.*, 2010]. This indicates that the effect of changes due to LULCC in plant productivity and biomass turnover, which are accounted for in models but not in the bookkeeping approach, is of secondary importance for the simulated C balance.

ESMs perform poorly in respect to global soil carbon stocks and turnover times, irrespective of the complexity of the decomposition model [*Todd-Brown et al.*, 2013]. *Todd-Brown et al.* [2013] found a 5.9-fold variation in global soil carbon stocks and 3.6 variation in turnover times of soil carbon among ESMs, with the majority of simulated stock and rates lying outside the observed range. Although soil carbon decomposition is recognized as a major source of uncertainty in the estimation of the LULCC flux [*Houghton et al.*, 2012], it is usually not addressed.

Here we assess the uncertainty in LULCC emissions for a given LULCC scenario due to treatment of initial land cover, direct emissions, and decomposition by rerunning a subset of the CMIP5 experiments performed with the MPI- ESM with the carbon cycle and vegetation distribution component of MPI-ESM (CBALANCE).

2. Methods

We performed simulations with CBALANCE in which we altered (1) initial land cover, (2) the parameter controlling the fraction of directly emitted carbon, and (3) the representation of decomposition. In the following, we give an overview of the land model of MPI-ESM, a detailed description of the two decomposition submodels used, the representation of LULCC, and the simulations we performed.

A detailed evaluation of the two decomposition models using data from a soil warming experiment and a global soil carbon data set, as well as an analysis of the apparent residence times of soil carbon following *Todd-Brown et al.* [2013], can be found in the supporting information (Texts S2 and S3). Here we only briefly document the methods and the data used.

2.1. MPI-ESM: Land Component

The Max Planck Institute Earth System Model (MPI-ESM) [*Giorgetta et al.*, 2013] incorporates a terrestrial component (JSBACH) which provides the lower atmospheric boundary conditions over land and simulates ecosystems responses to changes in climate and how these responses in turn influence the exchange of carbon, trace gases, and other species. The land component is increasingly used as a stand alone model for carbon cycle related applications spanning the quantification of LULCC emissions [*Reick et al.*, 2010], nutrient dynamics [*Goll et al.*, 2012], fire [*Brücher et al.*, 2014], and plant adaptation [*Verheijen et al.*, 2012]. The structure of the terrestrial carbon cycle of MPI-ESM is shown in Figure 1a and described in detail in *Goll et al.* [2012].

In the following we focus on the two different representation of decomposition and on the representation of land cover change.

2.1.1. The Reference Decomposition Model (CTL)

The structure of CTL is derived from the commonly used CENTURY model [*Parton et al.*, 1993]. Dead organic matter is represented by two litter pools, lignified and lignin free, and one pool for slowly decomposing soil organic matter [*Goll et al.*, 2012]. The temperature dependence of decomposition is described by a Q_{10} equation ($Q_{10} = 1.8$) [*Lloyd and Taylor*, 1994], combined with a linear dependence on relative soil moisture content [*Knorr*, 2000]. At reference conditions ($T_{soil} = 0°C$ and soil moisture at field capacity), the turnover of the lignin-free litter lies between 1.8 and 2.5 years depending on the plant functional type (PFT); the turnover time of woody litter is 30 years. The turnover time of slowly decomposing soil organic matter (100 years) has been the subject to calibration during the MPI-ESM development, where, similar to the fraction of direct LULCC emissions, it is adjusted to minimize biases in historical land carbon balance.

2.1.2. Implementation of YASSO

The decomposition model YASSO [*Tuomi et al.*, 2008, 2009, 2011a, 2011b] is based on litter bag experiment and soil carbon measurements and was evaluated on site to regional scale [*Thum et al.*, 2011; *Karhu et al.*, 2012; *Rantakari et al.*, 2012; *Lu et al.*, 2013; *Ortiz et al.*, 2013]. Here we briefly summarize the structure of YASSO and specific details of its implementation into JSBACH (a detailed description of the implementation in the present study is given in the supporting information Text S1). In YASSO, litter is separated into four pools representing groups of chemical compounds (*j*).

Each of these compound groups has its own decomposition rate independent of litter type or plant species. In the case of woody litter, the decomposition rates of these four pools decrease with an increasing size of
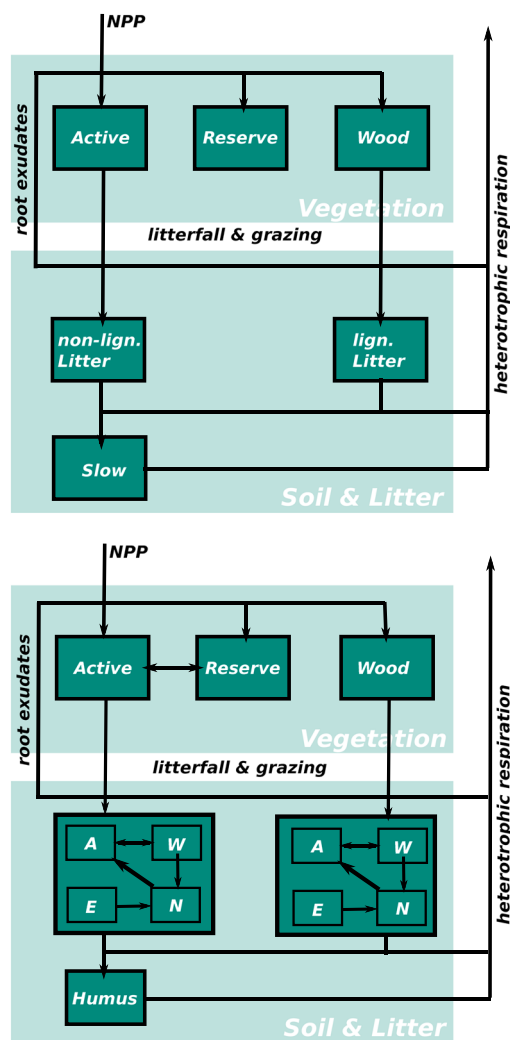
Figure 1. The structure of carbon cycle with the original (CTL) and the alternative decomposition model (YASSO). NPP is allocated to the three plant compartments: active (leaves and nonlignified tissue), wood (stems, branches, and coarse roots), and reserve (carbohydrates). A fraction of the NPP enters the soil system as root exudates. By litterfall and grazing carbon is transferred from the plant compartments to soil and litter. In CTL litter is represented by a pool for nonlignified litter and lignified litter (including fast decomposing soil organic matter), respectively. Slow decomposing organic matter is represented by a single pool. When carbon is transferred from the litter pools to the slow pool, a certain fraction is considered heterotrophic respiration. In YASSO, soil organic matter and litter is represented by four pools, representing groups of different chemical compounds, for each litter class and a single humus pool. These groups are defined and measured based on a common chemical extraction procedure: soluble in acid (A), in water (W), in ethanol (E), or nonsoluble (N).

the litter. In addition to these four pools, there is a humus pool that receives a fraction of the decomposition products of the more labile pools.

The dependence of decomposition on air temperature is described by optimum curve [*Tuomi et al.*, 2008], combined with a $k(P) = 1 - e^{-1.2*P}$ dependence on precipitation [*Tuomi et al.*, 2009].

2.1.3. Land Use and Land Cover Change

The representation of LULCC is described in detail by *Reick et al.* [2013]. Here we briefly summarize the effect of land cover change on the carbon cycle, which is based on the work by *Pongratz et al.* [2009a]. Wood harvest and land cover transitions are read in from reconstructions by *Hurtt et al.* [2011]. The land cover data contains information on the gross transitions of unspecified natural land to agricultural land relocating carbon between pools as follows. The aboveground vegetation carbon of cover types with decreasing area is either directly released to the atmosphere or relocated to the pools for decomposing matter. Direct release of carbon into the atmosphere simulates removal from the terrestrial system through mechanisms like fire, short-lived paper products, and harvesting method. This direct release fraction (f_a) was initially set to 0.5 [*Pongratz et al.*, 2009a]; however, more recent calibration efforts placed it at 0.8 [*Giorgetta et al.*, 2013]. The remaining carbon ($1 - f_a$) is relocated to either nonwoody or woody decomposition pools. Long-term product pools have been shown to have a negligible impact on model results [*Parida et al.*, 2011] and are excluded for simplicity in this model.

2.2. Model Configurations and Simulations

We ran the carbon cycle and vegetation distribution component of MPI-ESM, CBALANCE, independently from the rest of the model following *Goll et al.* [2012]. CBALANCE includes wind and fire damage, land cover changes by land use and by natural vegetation dynamics, and harvest. CBALANCE is capable of reproducing exactly the results of the coupled MPI-ESM model with respect to the land carbon cycle and land vegetation cover, when it is forced by the output from the coupled model. The modeling setup ignores feedbacks between land processes and climate, because climate conditions are prescribed from full MPI-ESM simulation when running CBALONE. However, the biochemical feed-

backs were not accounted for in the CMIP5 simulations [*Taylor et al.*, 2012], and the biophysical effects of changes in land cover on the historical LULCC flux in MPI-ESM are marginal [*Brovkin et al.*, 2013a]. Thus, the resulting inconsistencies between climate and land surface should not principally change the results of the present study.

Table 1. List of Model Configurations[a]

Acronym	Decomposition	Land Cover	f_a
CTL_DYN_HIGH	CTL	computed	0.8
CTL_DYN_LOW	CTL	computed	0.3
CTL_REC_HIGH	CTL	reconstructed	0.8
CTL_REC_LOW	CTL	reconstructed	0.3
YASSO_DYN_HIGH	YASSO	computed	0.8
YASSO_DYN_LOW	YASSO	computed	0.3
YASSO_REC_HIGH	YASSO	reconstructed	0.8
YASSO_REC_LOW	YASSO	reconstructed	0.3

[a]The models differ in respect to decomposition model, natural land cover, and fraction of direct emissions. The configuration CTL_DYN_HIGH corresponds to the CMIP5 configuration.

The setup ensures that both decomposition modules are run with similar boundary conditions. CBALANCE is driven by net primary productivity (NPP), leaf area index, soil temperature, soil moisture, and wind speed. The YASSO decomposition module is driven by precipitation and air temperature, in contrast to CTL which uses soil moisture and soil temperature.

The forcing variables are extracted from simulations performed with MPI-ESM [*Giorgetta et al.*, 2013] under the framework of CMIP5 [*Taylor et al.*, 2012]. We use data from the historical ESM simulation aiming at the reconstruction of the climate from 1850 to 2005 under the influence of natural and anthropocentric forcings derived from observations. Further data spanning the years 2006–2200 were extracted from the projection simulation performed according to the Representative Concentration Pathway (RCP) 8.5 scenario. The CMIP5 simulations were conducted with prescribed atmospheric greenhouse gas concentrations (reflecting both anthropocentric and natural sources) [*Taylor et al.*, 2012]. The output variables of MPI-ESM simulations are provided for every land cover type at every grid independent of the prescribed land cover. Therefore, the initial land cover of simulations with the submodel can be different from the land cover used in the MPI-ESM simulations.

The forcing derived from the historical ESM simulation was extended by 100 years into the past, by randomly sampling the years 1850–1879 of the MPI-ESM simulation. This was done to ensure a comparison to state-of-the-art estimates of historical LULCC emissions which start in 1750. Land use change and harvest from 1750 to 2100 was prescribed using the reconstruction and projection for the RCP8.5 scenario by *Hurtt et al.* [2011] following the approach by *Reick et al.* [2013]. After 2100, land cover and harvest rates were kept on the level of 2100.

Sets of simulations from 1750 to 2200 were performed using eight different configurations of CBALANCE (Table 1). The different configurations use either CTL or YASSO decomposition model, either dynamically computed (DYN) or reconstructed (REC) natural land cover, and either a fraction of direct emission (f_a) of 0.3 (LOW) or 0.8 (HIGH). The reconstructions of preindustrial natural land cover is taken from *Pongratz et al.* [2008] based on the maps of potential vegetation by *Ramankutty and Foley* [1998]. The naming of the model configurations is decomposition_vegetation_f_a, for example, CTL_DYN_HIGH for the CMIP5 configuration of MPI-ESM. All simulations start from carbon stocks which were brought into equilibrium (less than 1% change in 30 year mean of global pools) beforehand using a repeated 30 year cycle of the forcing from the historical simulation by MPI-ESM and the respective model configuration.

To quantify the sources and sinks of carbon from LULCC, we performed a pair of simulations for each of the eight model configurations: one simulation with prescribed LULCC from *Hurtt et al.* [2011] and one simulation with constant land use and harvest of 1750. The LULCC flux is derived from the difference in the land carbon balance between the two simulations. Using the difference between a pair of simulations under identical LULCC and fossil fuel-influenced environmental conditions is the most common method to quantify the LULCC flux on global scale (D3 in *Pongratz et al.* [2014]). It allows a direct comparison of our results to previous studies on the factors influencing the sources and sinks of carbon from LULCC in MPI-ESM [*Schneck et al.*, 2015; *Wilkenskjeld et al.*, 2014].

The effect of initial land cover on LULCC in the historical period was assumed to be the difference between the simulations with reconstructed and dynamical natural land cover. Previous work has shown that variation in the LULCC flux due to the response of natural vegetation cover to climate change over the historical period is negligible [*Schneck et al.*, 2015]. We therefore interoperated differences between the DYC and REC simulations to be the result in differences in initial land cover. However, in the projected period (2010–2200) changes in the dynamically computed land cover start to affect the respective gross C fluxes significantly [*Schneck et al.*, 2015]. Therefore, our modeling setup is not suited to quantify the effects due to differences in the initial land cover in the projected period.

To quantify the effect of the parametrization of direct emission on the LULCC flux, we used the differences in the fluxes between model configurations which differ in f_a.

2.3. Evaluation of Decomposition Models

We evaluated the performance of the CTL and YASSO decomposition models to simulate the spatial variability of soil carbon stocks using estimates from the Harmonized World Soil Database (HWSD) (version 1.21). The analysis of spatial variability in soil carbon stocks is identical to the approach used by *Todd-Brown et al.* [2013] to evaluate the soil carbon simulations from 11 CMIP5 ESMs at both the grid and biome scales. This allows a direct comparison of model performances between studies. We conducted additional simulations in which we increased soil temperature by 5 K from April 2003 in the historical forcing from MPI-ESM to mimic the Barre Woods Soil Warming Experiment at Harvard Forest [*Melillo et al.*, 2003]. Details can be found in the supporting information.

3. Results and discussion

3.1. Evaluation of Decomposition Models

The comparison of simulated soil carbon distribution with the estimates from the HWSD shows a significantly better agreement between simulations and data with YASSO than with CTL (Figure 2 and Table S1). The CTL model simulates an inverse pattern of soil carbon compared to the HWSD and most of the CMIP5 models [*Todd-Brown et al.*, 2013]; soil carbon peaks in the midlatitudes across Asia, western North America, eastern Africa, southern South America, and southern coastal Australia. Using YASSO, this pattern is in good agreement with the HWSD ($r = 0.47$). As the inputs to the soil are identical for both simulations this effect can be attributed to the decomposition model solely.

The rather poor agreement between both model versions and HWSD on a grid scale (Table S1) could be due to uncertainties in the data, incorrect representation of drivers in the model (temperature, water, NPP, and LULCC), incorrect model structure (missing processes), or parametrization. The agreement of the simulated soil carbon stocks on the level of vegetation type is considerably better when YASSO is used (Figure S1) and, in general, better than on grid scale.

In summary, we find that YASSO performs significantly better than CTL in respect to the simulated soil carbon storage in MPI-ESM and slightly better in respect to the simulated stimulation of decomposition rates due to soil warming at a temperate forest site (Figure S1).

3.2. LULCC Fluxes

The simulated global net LULCC fluxes for different periods are shown in Table 2. All of the simulated LULCC fluxes lie in the uncertainty of estimates compiled by *Ciais et al.* [2013], except the decadal mean for the 1980s using the model configuration (YASSO_DYN_HIGH) with YASSO decomposition model, dynamically computed natural land cover, and high direct emissions.

Preindustrial natural land cover had the strongest effect on the net LULCC flux in our analysis. When reconstructed land cover is used, historical LULCC emissions are 42% lower than in the simulation with prognostic natural land cover (Table 2). Previous work has found that prognostic changes in natural land cover have a negligible effect on the historical LULCC emissions in MPI-ESM [*Schneck et al.*, 2015]. We found that the higher emissions in simulations with the prognostic land cover where the result of the 13% higher initial tree cover and, to a lesser extent, the 16% higher net primary productivity (NPP). The higher tree cover and elevated NPP results in 88 Pg C additionally stored in vegetation in 1750. The effect of the different land cover can also be seen in present-day soil carbon stocks, which differ globally among simulations by 18–20% (Figure S1).

On global scale, the differences in NPP, vegetation carbon, and land cover between simulations are well within the uncertainties in inventory-based and remote sensing-based estimates [*Ito*, 2011; *Ciais et al.*, 2013;
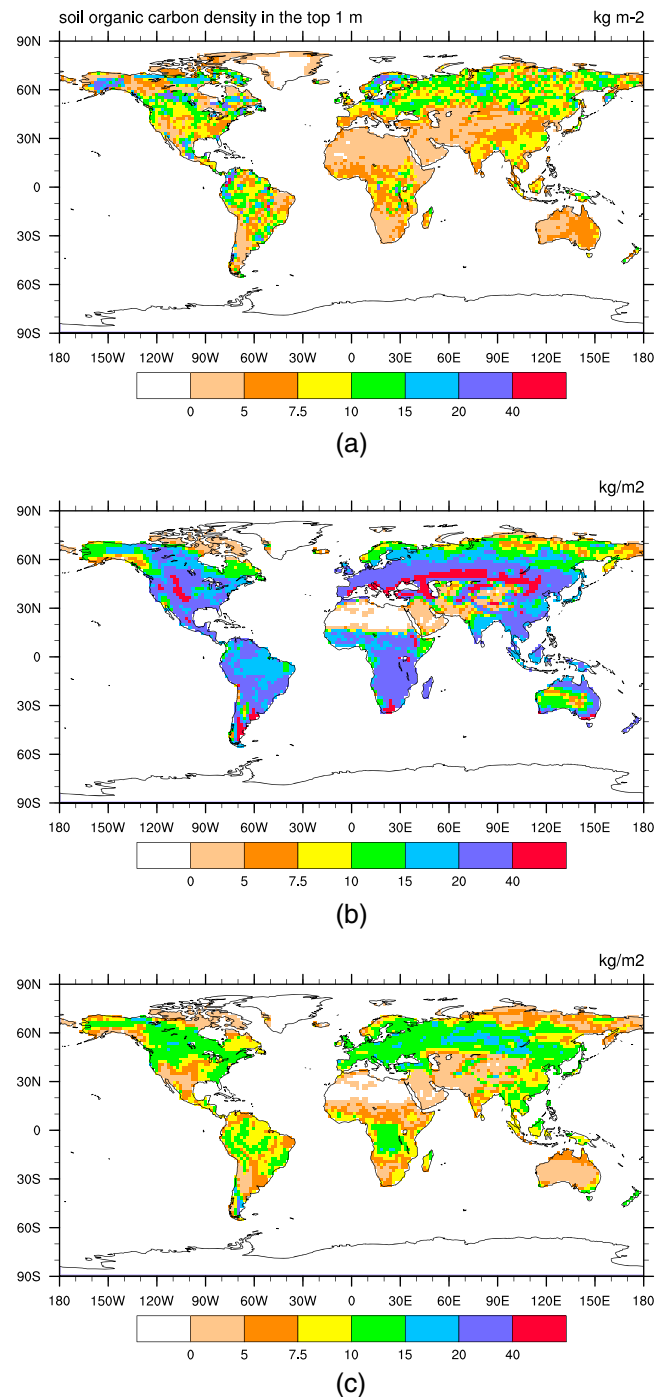
Figure 2. (a) Soil carbon in the top 1 m based on observations (HWSD) and total soil carbon as simulated by (b) CTL and (c) YASSO as means of the period 1986–2005.

Reick et al., 2013]. Nonetheless, a comparison to remote sensing-based vegetation continuous fields data set [*Hansen et al.*, 2003, 2007] indicates large regional biases in the prognostic tree cover [*Brovkin et al.*, 2013b]. Large biases in dynamically computed land cover are common features of the majority of global models [*Krinner et al.*, 2005], and continuous recalibrations of the dynamics of natural vegetation to changes in the terrestrial and atmospheric component of an ESM are difficult to maintain in constantly evolving models. In particular, biases in the subtropical regions can lead to large deviations in the LULCC flux due to high defor-estation rates [*Houghton et al.*, 2012]. In MPI-ESM, the positive bias in prognostic tree cover of Africa and South

Table 2. Accumulated Net LULCC Flux (Gt) Since the Industrial Revolution (1750–2010) and Decadal Means (Gt a^{-1}) for the Periods 1980–1989, 1990–1999, and 2000–2009

| | | CTL | | | | YASSO | | | |
| | | DYN | | REC | | DYN | | REC | |
Period	*Ciais et al.* [2013]	HIGH	LOW	HIGH	LOW	HIGH	LOW	HIGH	LOW
1750–2005	180 ± 80	248	188	145	106	264	246	150	144
1980s	1.4 ± 0.8	2.1	1.8	1.2	0.9	2.4	2.2	1.5	1.3
1990s	1.5 ± 0.8	2.0	1.8	1.0	0.8	2.1	2.1	1.2	1.2
2000s	1.1 ± 0.8	1.8	1.8	0.9	0.8	1.8	1.8	1.0	1.0

America alone is responsible for 87% of the differences in LULCC emissions between simulations (Figure 3). In these regions, remote sensing products and inventory-based estimates of vegetation carbon are restricted to a few decades and prone to large uncertainties [*Houghton et al.*, 2012]. The co-occurrence of grass and forest PFTs in savanna ecosystems is a major challenge for models as the mechanisms behind changes in land cover in semiarid drylands are multiple and general understanding is low [*Andela et al.*, 2013].

We found a strong interaction between the effect of decomposition model and parametrization of the direct emissions due to LULCC (Table 2). When high direct emissions are used, the choice of decomposition model has a marginal effect on LULCC fluxes. However, in case of low direct emission, when more carbon from LULCC is affected by decomposition, the representation of decomposition has a significant effect.

The effect of the parametrization of direct emission on LULCC fluxes differs in between decomposition models (Table 2). While in CTL historical LULCC emissions are 35% higher when a high fraction rather than a low fraction of direct emissions is assumed, in YASSO the emissions are only 5% higher. In CTL, the sign of the effect of historical LULCC on soil carbon depends on the parametrization of the fraction of direct emissions, while the parametrization has a small effect on soil losses in YASSO (Figure 4). The high sensitivity in CTL can be attributed to the higher apparent turnover time of soil C in YASSO of 13 years compared to 34 years in CTL (Text S3). The longer residence time results in a stronger delay of legacy emission relative to the direct emission in CTL compared to YASSO. The stronger the delay of legacy emission is, the more sensitive are emissions to the assumption about the fraction of direct emissions f_a. As the fraction of direct emissions implicitly represents the harvesting methods, the share between short-lived and long-lived wood products and burning practices, we conclude that their respective effects on LULCC fluxes depend on the assumed or modeled natural decomposition as well.

In summary, we show that regional biases in prognostic tree cover are solely responsible for the vast overestimation of LULCC emissions in the CMIP5 version of MPI-ESM (CTL_DYN_HIGH). Furthermore, we found
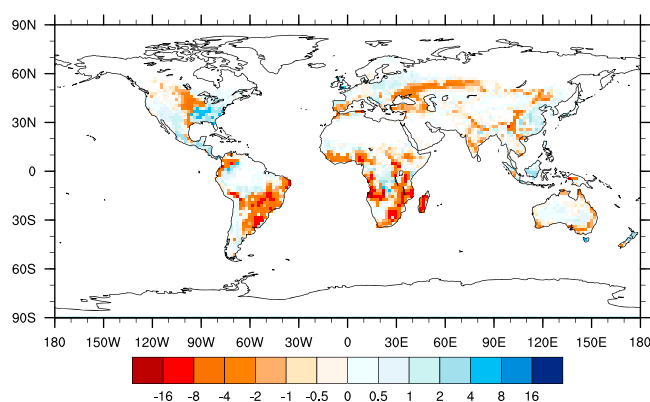

Figure 3. Differences in sources and sink due to historical LULCC (1750–2005) between simulations with reconstructed and dynamically computed land cover (kg m^{-2}). Negative values indicate higher emissions in simulations with dynamically computed land cover. The data is from the simulation with the CTL decomposition model and standard parametrization of direct emissions (HIGH).
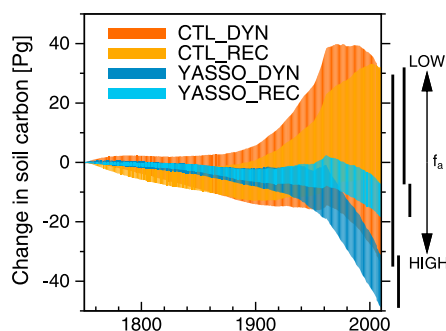
Figure 4. The sensitivity of emissions from soils (Pg C) due to LULCC to the parametrization of direct emissions from simulations using CTL (orange) or YASSO (blue). Natural land cover was either dynamically computed (dark) or from reconstructions (light). The shaded areas show the effect of f_a on the soil carbon with $f_a = 0.8$ leading to higher losses than $f_a = 0.3$.

uncertainties in decadal fluxes due the parametrization of decomposition and direct emissions which are up to 0.6 Pg C yr^{-1} (Table 2) 3 times as large as the uncertainties attributed previously to model and method by *Houghton et al.* [2012]. The actual uncertainties due to model and method are likely higher, as, for example, it was shown that the assumption about preferentially used land for pastures has a significant effect on LULCC emissions [*Reick et al.*, 2013; *Schneck et al.*, 2015], but it is not included in this uncertainty assessments. Thus, the overall accuracy of estimates of sinks and source due to LULCC is lower than usually suggested [*Houghton et al.*, 2012; *Ciais et al.*, 2013; *Pongratz et al.*, 2014]. In particular, the quantification of legacy emissions is a major source of uncertainty.

3.3. Terrestrial Carbon Balance

Historical period: 1750–2005: Observations show that the losses in terrestrial carbon storage due to LULCC are counterbalanced by increases in carbon storage elsewhere [*Ciais et al.*, 2013]. The processes driving the uptake of carbon are elusive, and the flux is usually called the residual sink or residual flux [*Ciais et al.*, 2013]. In ESMs carbon uptake is mainly driven by increases in NPP due the rise in atmospheric CO_2 concentrations, as well as by the lengthening of the vegetation period in temperature limited ecosystems due to warming [*Ciais et al.*, 2013]. However, in reality other processes might be involved which are usually omitted in ESMs, like forest management [*Erb et al.*, 2013] or nutrient dynamics [*Thomas et al.*, 2009; *Goll et al.*, 2012, 2014].

Like the LULCC flux, the residual flux in MPI-ESM is strongly affected by initial land cover and the representation of decomposition (Figure 5). The positive bias in the prognostic tree cover results in a historical (1750–2010) residual flux which is 39% (YASSO) to 53% (CTL) higher compared to simulations using reconstructed land cover. The higher tree cover results in higher fraction of global NPP being allocated to woody biomass which has a longer residence time than nonwoody material. Differences in NPP due to the difference
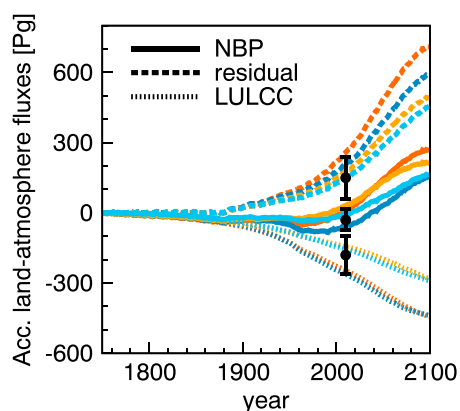

Figure 5. Accumulated land-atmosphere fluxes in simulations using either CTL (orange) or YASSO (blue) in comparison with estimates from *Ciais et al.* [2013] (dots). Shown are the net land atmosphere flux or net biome productivity (NBP), the LULCC flux, and the residual of both. In dark colors are simulations with natural land cover computed dynamically and in light colors are simulations with prescribed natural land cover. All simulations are with the standard parametrization of direct emissions (HIGH).

in the initial tree cover, as well as in changes in tree cover, itself are of secondary importance (not shown). The more pronounced effect in CTL compared to YASSO indicates that the difference in the apparent residence time between woody and nonwoody tissues is larger in CTL. The effect of the decomposition model itself on the historical residual flux is less than half as strong (−14 (REC) to −19% (DYN)) as the effect of initial land cover.

The uncertainty (90% confidence interval) in the estimate of net land carbon balance is large [*Ciais et al.*, 2013], and most of the simulated carbon fluxes are in the range of uncertainty. Nonetheless, the use of reconstructed initial land cover and the data-based decomposition model results in simulated gross fluxes which are significantly closer to the estimates than the CMIP5 version of the model.

Projected period: 2010–2200: For the 21st century, the simulated fluxes differ significantly between simulations (Figure 5). In this period, changes in the dynamically computed natural land cover start to affect the carbon cycle [*Schneck et al.*, 2015], preventing
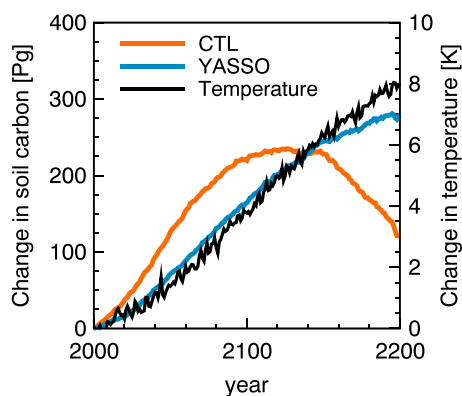
Figure 6. Projected change in global soil carbon simulated by CTL (orange) or YASSO (blue) and increase in surface temperature (black) under the RCP 8.5 scenario. All simulations are with the standard parametrization of direct emissions (HIGH).

conclusions about the effect of initial land cover on the carbon cycle from our simulation setup. Therefore, we focus on the representation of decomposition which we found to exert a strong effect on the net carbon flux.

The difference in the increase in terrestrial carbon storage between the two decomposition models (Figure 5) is comparable to effect of nitrogen and phosphorus cycling on the terrestrial carbon balance in an earlier version of MPI-ESM [*Goll et al.*, 2012]. The mutual importance of the representation of decomposition and nutrient limitation was previously shown for the Carnegie-Ames-Stanford Approach with Carbon-Nitrogen-Phosphorus model *Exbrayat et al.* [2013]. A comparison of nitrogen needed to support the increase in carbon storage simulated by the CMIP5 version of MPI-ESM (CTL_DYN_HIGH) with actual nitrogen supply showed that the simulated increase in terrestrial carbon storage is to a large degree not supported by available nitrogen [*Zaehle et al.*, 2015]. The discrepancy between needed and available nitrogen was driven nearly entirely by the increase in soil carbon storage. The significantly lower increase in soil carbon simulated by YASSO compared to CTL translates to a reduction of the discrepancy by 65%.

The spatial pattern of changes in soil carbon is hardly affected by the decomposition model itself, despite the large differences in present day stocks (Figure 2). The pattern of change is mainly driven by changes in NPP, only the fraction of NPP which is stored in soils is controlled by decomposition. As YASSO has a faster apparent turnover of soil carbon than CTL, the increase in soil carbon is smaller in YASSO (Text S3).

We extended the simulation to the year 2200 keeping LULCC constant to analyze the effect of strong warming on decomposition. The simulations reveal contrasting evolutions of global soil carbon between the decomposition models when temperature rise more than 6 K (Figure 6). While CTL simulates a decline in soil C, YASSO simulates a continuous increase. The warming experiment (Text S4) showed that the response of decomposition to warming on a decadal time scale is likely overestimated in CTL. However, under strong warming, the difference in the size of initial soil carbon stocks and to a lesser extent in the temperature response functions between CTL and YASSO is responsible for the contrasting evolution. In CTL a Q_{10} formulation is used, while in YASSO an optimum curve is used which accounts for a downregulation of decomposition at high temperatures. A downregulation of decomposition at high temperature, in general, is supported by experimental evidence, but current understanding is low [*Wei et al.*, 2014]. As changes in soil respiration scale with substrate availability, the higher (260%) initial soil carbon stocks in CTL is mainly responsible for higher soil carbon losses.

4. Conclusions

Here we show that initial tree cover is a critical factor in the quantification of the net historical LULCC flux, driving the overestimation of the LULCC fluxes in MPI-ESM. Other aspects directly related to LULCC like the representation of shifting cultivation [*Wilkenskjeld et al.*, 2014], forest regrowth [*Schneck et al.*, 2015], or assumption about the conversion of pastures [*Reick et al.*, 2013] are of secondary importance. We show that the spread in simulated net LULCC fluxes between simulations using different initial natural land cover is comparable to the spread between 13 recent estimates of historical and present-day LULCC fluxes, which is base on multiple approaches and terminologies of LULCC [*Houghton et al.*, 2012; *Pongratz et al.*, 2014]. As other models with dynamically computed land cover show comparable biases in land cover [*McGuire et al.*, 2001; *Krinner et al.*, 2005], we discourage the use of dynamically computed land cover in LULCC studies, in general, as long as a realistic land cover cannot be ensured in these models.

The effect of LULCC on the carbon balance of soils strongly depends on the representation of decomposition and the parametrization of direct emissions. We find an uncertainty in the total LULCC flux on decadal time scale of 0.6 Pg C yr^{-1} (Table 2) due to the parametrization of decomposition and direct emissions, which is

3 times as large as the uncertainties attributed previously to model and method in general [*Houghton et al.*, 2012]. A part of the uncertainty is likely related to the long (34 year) apparent turnover time of soil organic matter in the standard decomposition model in MPI-ESM. The use of the decomposition model with a faster (13 year) apparent turnover time substantially reduces the sensitivity of the LULCC flux to the parametrization of direct emissions. However, the turnover time of YASSO lies outside the range of empirical based estimates which are 18.5–32 years [*Raich and Schlesinger*, 1992; *Amundson*, 2001]. Likely due to the more extensive calibration effort invested in YASSO development [*Tuomi et al.*, 2008, 2009, 2011a], we observed a significant improvement in simulating LULCC and residual fluxes, as well as present-day soil carbon distribution.

We attribute the poor performance of MPI-ESM with respect to the gross carbon fluxes to the practice of calibrating the net land carbon balance, i. e., the residence time of slowly decomposing organic matter in CTL and fraction of direct emissions, to provide realistic boundary conditions for the climate component of the ESM over the historical period [*Giorgetta et al.*, 2013], whereas the subcomponents of the carbon balance lack a thorough evaluation using observations. The calibration of components of ESM for the biogeochemical cycles to meet a certain target value has to be assumed a common procedure if it is not to be regarded as a mere coincidence that models regularly meet prominent properties of the system, for example, the net carbon balance, while the underlying components deviate strongly from observations [*Anav et al.*, 2013; *Todd-Brown et al.*, 2013]. This has far reaching implications for the applicability of land components of ESMs outside their primary field of application. In line with recent studies [*Anav et al.*, 2013; *Peñuelas*, 2013; *Prentice et al.*, 2014; *Todd-Brown et al.*, 2014; *Medlyn et al.*, 2015], we argue for the thorough use of observational data to design, constrain, and evaluate each subcomponent of the carbon cycle to ensure the reliability of models.

References

Amundson, R. (2001), The carbon budget in soils, *Ann. Rev. Earth Planet. Sci.*, *29*, 535–562, doi:10.1146/annurev.earth.29.1.535.

Anav, A., P. Friedlingstein, M. Kidston, L. Bopp, P. Ciais, P. Cox, C. Jones, M. Jung, R. Myneni, and Z. Zhu (2013), Evaluating the land and ocean components of the global carbon cycle in the CMIP5 Earth system models, *J. Clim.*, *26*, 6801–6843, doi:10.1175/JCLI-D-12-00417.1.

Andela, N., Y. Y. Liu, a. I. J. M. v. Dijk, R. a. M. d. Jeu, and T. R. McVicar (2013), Global changes in dryland vegetation dynamics (1988–2008) assessed by satellite remote sensing: Comparing a new passive microwave vegetation density record with reflective greenness data, *Biogeosciences*, *10*(10), 6657–6676, doi:10.5194/bg-10-6657-2013.

Arora, V. K., and G. J. Boer (2010), Uncertainties in the 20th century carbon budget associated with land use change, *Global Change Biol.*, *16*(12), 3327–3348, doi:10.1111/j.1365-2486.2010.02202.x.

Brovkin, V., et al. (2013a), Effect of anthropogenic land-use and land-cover changes on climate and land carbon storage in CMIP5 projections for the twenty-first century, *J. Clim.*, *26*(18), 6859–6881, doi:10.1175/JCLI-D-12-00623.1.

Brovkin, V., L. Boysen, T. Raddatz, V. Gayler, A. Loew, and M. Claussen (2013b), Evaluation of vegetation cover and land-surface albedo in MPI-ESM CMIP5 simulations, *J. Adv. Model. Earth Syst.*, *5*(1), 48–57, doi:10.1029/2012MS000169.

Brücher, T., V. Brovkin, S. Kloster, J. R. Marlon, and M. J. Power (2014), Comparing modelled fire dynamics with charcoal records for the Holocene, *Clim. Past*, *10*, 811–824, doi:10.5194/cp-10-811-2014.

Ciais, P., et al. (2013), Carbon and other biogeochemical cycles, in *Climate Change 2013: The Physical Science Basis: Contribution of Working Group I to the Fifth Assessment Report of the Intergovernmental Panel on Climate Change*, edited by T. Stocker et al., chap. Carbon, pp. 465–570, Cambridge Univ. Press, Cambridge, U. K., and New York.

Cox, P. M. (2001), Description of the "TRIFFID" dynamic global vegetation model. Hadley Centre technical note 24, *Tech. Rep.*, Hadley Centre, Met Office, Berks, U. K.

Delworth, T. L., et al. (2012), Simulated climate and climate change in the GFDL CM2.5 high-resolution coupled climate model, *J. Clim.*, *25*(8), 2755–2781, doi:10.1175/JCLI-D-11-00316.1.

de Noblet-Ducoudré, N., et al. (2012), Determining robust impacts of land-use-induced land cover changes on surface climate over North America and Eurasia: Results from the first set of LUCID experiments, *J. Clim.*, *25*(9), 3261–3281, doi:10.1175/JCLI-D-11-00338.1.

Dunee, J., et al. (2013), GFDL's ESM2 global coupled climate-carbon earth system models. Part II: Carbon system formulation and baseline simulation characteristics, *J. Clim.*, *26*(7), 2247–2267, doi:10.1175/JCLI-D-12-00150.1.

Erb, K.-H., T. Kastner, S. Luyssaert, R. a. Houghton, T. Kuemmerle, P. Olofsson, and H. Haberl (2013), Bias in the attribution of forest carbon sinks, *Nat. Clim. Change*, *3*(10), 854–856, doi:10.1038/nclimate2004.

Exbrayat, J.-F., A. J. Pitman, Q. Zhang, G. Abramowitz, and Y.-P. Wang (2013), Examining soil carbon uncertainty in a global model: Response of microbial decomposition to temperature, moisture and nutrient limitation, *Biogeosciences*, *10*(11), 7095–7108, doi:10.5194/bg-10-7095-2013.

Fearnside, P. M. (2000), Global warming and tropical land-use change: Greenhouse gas emissions from biomass burning, decomposition and soils in forest conversion, shifting cultivation and secondary vegetation, *Clim. Change*, *46*, 115–158.

Giorgetta, M. A., et al. (2013), Climate and carbon cycle changes from 1850 to 2100 in MPI-ESM simulations for the coupled model intercomparison project phase 5, *J. Adv. Model. Earth Syst.*, *5*, 1–26, doi:10.1002/jame.20038.

Goll, D. S., V. Brovkin, B. R. Parida, C. H. Reick, J. Kattge, P. B. Reich, P. M. van Bodegom, and U. Niinemets (2012), Nutrient limitation reduces land carbon uptake in simulations with a model of combined carbon, nitrogen and phosphorus cycling, *Biogeosciences*, *9*(9), 3547–3569, doi:10.5194/bg-9-3547-2012.

Goll, D. S., N. Moosdorf, J. Hartmann, and V. Brovkin (2014), Climate-driven changes in chemical weathering and associated phosphorus release since 1850: Implications for the land carbon balance, *Geophys. Res. Lett.*, *41*, 3553–3558, doi:10.1002/2014GL059471.

Hansen, M. C., R. S. DeFries, J. R. G. Townshend, M. Carroll, C. Dimiceli, and R. a. Sohlberg (2003), Global percent tree cover at a spatial resolution of 500 meters: First results of the MODIS vegetation continuous fields algorithm, *Earth Interact.*, *7*(10), 1–15, doi:10.1175/1087-3562(2003)007<0001:GPTCAA>2.0.CO;2.

Hansen, M. C., R. S. DeFries, J. R. Townshend, M. Carroll, C. Dimiceli, and R. Sohlberg (2007), *Vegetation Continuous Fields MOD44B, 2011 Percent Tree Cover, Collection 4*, Univ. of Maryland, College Parl, MD.

Houghton, R. A., J. E. Hobbie, J. M. Melillo, B. Moore, B. J. Peterson, G. E. Shaver, and G. M. Woodwell (1983), Changes in the carbon content of terrestrial biota and soils between 1860 and 1980: A net release of CO2 to the atmosphere, *Ecol. Monogr.*, *53*(3), 235–262.

Houghton, R. A., J. I. House, J. Pongratz, G. R. van der Werf, R. S. DeFries, M. C. Hansen, C. Le Quéré, and N. Ramankutty (2012), Carbon emissions from land use and land-cover change, *Biogeosciences*, *9*(12), 5125–5142, doi:10.5194/bg-9-5125-2012.

Hurtt, G. C., et al. (2011), Harmonization of land-use scenarios for the period 1500-2100: 600 years of global gridded annual land-use transitions, wood harvest, and resulting secondary lands, *Clim. Change*, *109*(1–2), 117–161, doi:10.1007/s10584-011-0153-2.

Ito, A. (2011), A historical meta-analysis of global terrestrial net primary productivity: Are estimates converging?, *Global Change Biol.*, *17*(10), 3161–3175, doi:10.1111/j.1365-2486.2011.02450.x.

Ji, D., et al. (2014), Description and basic evaluation of BNU-ESM version 1, *Geosci. Model Dev. Discuss.*, *7*(2), 1601–1647, doi:10.5194/gmdd-7-1601-2014.

Karhu, K., A. I. Gärdenäs, J. Heikkinen, P. Vanhala, M. Tuomi, and J. Liski (2012), Impacts of organic amendments on carbon stocks of an agricultural soil Comparison of model-simulations to measurements, *Geoderma*, *189-190*, 606–616, doi:10.1016/j.geoderma.2012.06.007.

Knorr, W. (2000), Annual and interannual CO_2 exchanges of the terrestrial biosphere : Process-based simulations and uncertainties, *Global Ecol. Biogeogr.*, *9*(3), 225–252.

Krinner, G., N. Viovy, N. de Noblet-Ducoudré, J. Ogée, J. Polcher, P. Friedlingstein, P. Ciais, S. Sitch, and I. C. Prentice (2005), A dynamic global vegetation model for studies of the coupled atmosphere-biosphere system, *Global Biogeochem. Cycles*, *19*(1), GB1015, doi:10.1029/2003GB002199.

Lawrence, P. J., et al. (2012), Simulating the biogeochemical and biogeophysical impacts of transient land cover change and Wood Harvest in the Community Climate System Model (CCSM4) from 1850 to 2100, *J. Clim.*, *25*(9), 3071–3095, doi:10.1175/JCLI-D-11-00256.1.

Lloyd, J., and J. A. Taylor (1994), *On the Temperature Dependence of Soil Respiration*, *8*(3), 315–323.

Lu, N., J. Liski, R. Y. Chang, A. Akujärvi, X. Wu, T. T. Jin, Y. F. Wang, and B. J. Fu (2013), Soil organic carbon dynamics of black locust plantations in the middle Loess Plateau area of China, *Biogeosciences*, *10*(11), 7053–7063, doi:10.5194/bg-10-7053-2013.

McGuire, A. D., et al. (2001), Carbon balance of the terrestrial biosphere in the Twentieth Century: Analyses of CO_2, climate and land use effects with four process-based ecosystem models, *Global Biogeochem. Cycles*, *15*(1), 183–206, doi:10.1029/2000GB001298.

Medlyn, B., et al. (2015), Using ecosystem experiments to improve vegetation models: Lessons learnt from the free-air CO_2 enrichment model-data synthesis, *Nat. Clim. Change*, *5*, 528Ű–534.

Melillo, J. M., P. A. Steudler, and J. Mohan (2003), Barre woods soil warming experiment at Harvard Forest since 2001, *Tech. Rep.*, Harvard Forest Data Archieve: HF018.

Ortiz, C. A., J. Liski, A. I. Gärdenäs, A. Lehtonen, M. Lundblad, J. Stendahl, G. I. Ågren, and E. Karltun (2013), Soil organic carbon stock changes in Swedish forest soils — A comparison of uncertainties and their sources through a national inventory and two simulation models, *Ecol. Modell.*, *251*, 221–231, doi:10.1016/j.ecolmodel.2012.12.017.

Parida, B. R., C. H. Reick, J. Kattge, and D. S. Goll (2011), Coupled nitrogen-carbon cycle simulations for the 21st century with JSBACH-CN and progressive nitrogen limitation, *Rep. Earth Syst. Sci.*, *92*(2011).

Parton, W. J., et al. (1993), Observations and modeling of biomass and soil organic matter dynamics for the grassland biome worldwide, *Glob. Biogeochem. Cycles*, *7*, 785–809, doi:10.1029/93GB02042.

Peñuelas, J. (2013), Human-induced nitrogen-phosphorus imbalances alter natural and managed ecosystems across the globe, *Nat. Commun.*, *4*, 2934, doi:10.1038/ncomms3934.

Pitman, A. J., et al. (2009), Uncertainties in climate responses to past land cover change: First results from the LUCID intercomparison study, *Geophys. Res. Lett.*, *36*(14), doi:10.1029/2009GL039076.

Pitman, A. J., et al. (2012), Effects of land cover change on temperature and rainfall extremes in multi-model ensemble simulations, *Earth Syst. Dynam.*, *3*(2), 213–231, doi:10.5194/esd-3-213-2012.

Pongratz, J., C. Reick, T. Raddatz, and M. Claussen (2008), A reconstruction of global agricultural areas and land cover for the last millennium, *Global Biogeochem. Cycles*, *22*(3), GB3018, doi:10.1029/2007GB003153.

Pongratz, J., C. H. Reick, T. Raddatz, and M. Claussen (2009a), Effects of anthropogenic land cover change on the carbon cycle of the last millennium, *Global Biogeochem. Cycles*, *23*, doi:10.1029/2009GB003488.

Pongratz, J., T. Raddatz, C. H. Reick, M. Esch, and M. Claussen (2009b), Radiative forcing from anthropogenic land cover change since A.D. 800, *Geophys. Res. Lett.*, *36*(2), L02709, doi:10.1029/2008GL036394.

Pongratz, J., C. H. Reick, T. Raddatz, and M. Claussen (2010), Biogeophysical versus biogeochemical climate response to historical anthropogenic land cover change, *Geophys. Res. Lett.*, *37*(8), L08702, doi:10.1029/2010GL043010.

Pongratz, J., K. Caldeira, C. H. Reick, and M. Claussen (2011), Coupled climate-carbon simulations indicate minor global effects of wars and epidemics on atmospheric CO_2 between AD 800 and 1850, *The Holocene*, *21*(5), 843–851, doi:10.1177/0959683610386981.

Pongratz, J., C. H. Reick, R. A. Houghton, and J. I. House (2014), Terminology as a key uncertainty in net land use and land cover change carbon flux estimates, *Earth Syst. Dynam.*, *5*(1), 177–195, doi:10.5194/esd-5-177-2014.

Prentice, I. C., X. Liang, B. E. Medlyn, and Y.-P. Wang (2014), Reliable, robust and realistic: The three R's of next-generation land surface modelling, *Atmos. Chem. Phys. Discuss.*, *14*(17), 24,811–24,861, doi:10.5194/acpd-14-24811-2014.

Thomas, Q. R., C. D. Canham, K. C. Weathers, and C. L. Goodale (2009), Increased tree carbon storage in response to nitrogen deposition in the U.S., *Nat. Geosci.*, *3*(1), 13–17.

Ramankutty, N., and J. A. Foley (1998), Characterizing patterns of global land use: An analysis of global croplands data, *Global Biogeochem. Cycles*, *12*(4), 667–685, doi:10.1029/98GB02512.

Ramankutty, N., H. K. Gibbs, F. Achard, R. Defries, J. A. Foley, and R. A. Houghton (2007), Challenges to estimating carbon emissions from tropical deforestation, *Global Change Biol.*, *13*(1), 51–66, doi:10.1111/j.1365-2486.2006.01272.x.

Rantakari, M., et al. (2012), The Yasso07 soil carbon model testing against repeated soil carbon inventory, *For. Ecol. Manage.*, *286*, 137–147, doi:10.1016/j.foreco.2012.08.041.

Reick, C. H., T. Raddatz, J. Pongratz, and M. Claussen (2010), Contribution of anthropogenic land cover change emissions to pre-industrial atmospheric CO_2, *Tellus B*, *62*(5), 329–336, doi:10.1111/j.1600-0889.2010.00479.x.

Reick, C. H., T. Raddatz, V. Brovkin, and V. Gayler (2013), Representation of natural and anthropogenic land cover change in MPI-ESM, *J. Adv. Model. Earth Syst.*, *5*(3), 459–482, doi:10.1002/jame.20022.

Raich, J. W., and W. H. Schlesinger (1992), The global carbon dioxide flux in soil respiration and its relationship to vegetation and climate, *Tellus*, *44*, 81–99.

Sato, H., A. Itoh, and T. Kohyama (2007), SEIBDGVM: A new dynamic global vegetation model using a spatially explicit individual-based approach, *Ecol. Modell.*, *200*(3–4), 279–307, doi:10.1016/j.ecolmodel.2006.09.006.

Schneck, R., C. H. Reick, J. Pongratz, and V. Gayler (2015), The mutual importance of anthropogenically and climate induced changes in global vegetation cover for future land carbon emissions in the MPI-ESM CMIP5 simulations, *Global Biogeochem. Cycles*, 29, doi:10.1002/2014GB004959.

Shevliakova, E., R. J. Stouffer, S. Malyshev, J. P. Krasting, G. C. Hurtt, and S. W. Pacala (2013), Historical warming reduced due to enhanced land carbon uptake, *Proc. Nat. Acad. Sci. U.S.A.*, 42, 16, 730–16,735, doi:10.1073/pnas.1314047110.

Sitch, S., et al. (2003), Evaluation of ecosystem dynamics, plant geography and terrestrial carbon cycling in the LPJ dynamic global vegetation model, *Global Change Biol.*, 9(2), 161–185, doi:10.1046/j.1365-2486.2003.00569.x.

Strassmann, K. M., F. Joos, and G. Fischer (2008), Simulating effects of land use changes on carbon fluxes: Past contributions to atmospheric CO_2 increases and future commitments due to losses of terrestrial sink capacity, *Tellus B*, 60(4), 583–603, doi:10.1111/j.1600-0889.2008.00340.x.

Taylor, K. E., R. J. Stouffer, and G. A. Meehl (2012), An overview of CMIP5 and the experiment design, *Bull. Am. Meteorol. Soc.*, 93(4), 485–498, doi:10.1175/BAMS-D-11-00094.1.

Thum, T., et al. (2011), Soil carbon model alternatives for ECHAM5/JSBACH climate model: Evaluation and impacts on global carbon cycle estimates, *J. Geophys. Res.*, 116, G02028, doi:10.1029/2010JG001612.

Todd-Brown, K. E. O., J. T. Randerson, W. M. Post, F. M. Hoffman, C. Tarnocai, E. A. G. Schuur, and S. D. Allison (2013), Causes of variation in soil carbon simulations from CMIP5 Earth system models and comparison with observations, *Biogeosciences*, 10(3), 1717–1736, doi:10.5194/bg-10-1717-2013.

Todd-Brown, K. E. O., et al. (2014), Changes in soil organic carbon storage predicted by Earth system models during the 21st century, *Biogeosciences*, 11(8), 2341–2356, doi:10.5194/bg-11-2341-2014.

Tuomi, M., P. Vanhala, K. Karhu, H. Fritze, and J. Liski (2008), Heterotrophic soil respiration comparison of different models describing its temperature dependence, *Ecol. Modell.*, 211(1–2), 182–190, doi:10.1016/j.ecolmodel.2007.09.003.

Tuomi, M., T. Thum, H. Järvinen, S. Fronzek, B. Berg, M. Harmon, J. Trofymow, S. Sevanto, and J. Liski (2009), Leaf litter decomposition estimates of global variability based on Yasso07 model, *Ecol. Modell.*, 220(23), 3362–3371, doi:10.1016/j.ecolmodel.2009.05.016.

Tuomi, M., R. Laiho, A. Repo, and J. Liski (2011a), Wood decomposition model for boreal forests, *Ecol. Modell.*, 222(3), 709–718, doi:10.1016/j.ecolmodel.2010.10.025.

Tuomi, M., J. Rasinmäki, A. Repo, P. Vanhala, and J. Liski (2011b), Soil carbon model Yasso07 graphical user interface, *Environ. Modell. Software*, 26(11), doi:10.1016/j.envsoft.2011.05.009.

van der Werf, G. R. (2010), Global fire emissions and the contribution of deforestation, savanna, forest, agricultural, and peat fires (1997–2009), *Atmos. Chem. Phys.*, 10(23), 11,707–11,735, doi:10.5194/acp-10-11707-2010.

Verheijen, L. M., V. Brovkin, R. Aerts, G. Bönisch, J. H. C. Cornelissen, J. Kattge, P. B. Reich, I. J. Wright, and P. M. van Bodegom (2012), Impacts of trait variation through observed trait-climate relationships on performance of a representative Earth System model: A conceptual analysis, *Biogeosciences Discuss.*, 9(12), 18,907–18,950, doi:10.5194/bgd-9-18907-2012.

Watanabe, S., et al. (2011), MIROC-ESM 2010: model description and basic results of CMIP5-20c3m experiments, *Geosci. Model Dev.*, 4(4), 845–872, doi:10.5194/gmd-4-845-2011.

Wei, H., B. Guenet, S. Vicca, N. Nunan, H. AbdElgawad, V. Pouteau, W. Shen, and I. A. Janssens (2014), Thermal acclimation of organic matter decomposition in an artificial forest soil is related to shifts in microbial community structure, *Soil Biol. Biochem.*, 71, 1–12, doi:10.1016/j.soilbio.2014.01.003.

Wilkenskjeld, S., S. Kloster, J. Pongratz, T. Raddatz, and C. Reick (2014), Comparing the influence of net and gross anthropogenic land use and land cover changes on the carbon cycle in the MPI-ESM, *Biogeosciences*, 11, 4817–4828, doi:10.5194/bg-11-4817-2014.

Zaehle, S., C. D. Jones, B. Z. Houlton, J.-F. Lamarque, and E. Robertson (2015), Nitrogen availability reduces CMIP5 projections of 21St century land carbon uptake, *J. Clim.*, doi:10.1175/JCLI-D-13-00776.1.